Measurement of electroweak-boson production in pp, p–Pb, and Pb–Pb collisions with ALICE at the LHC

Shingo Sakai for the ALICE collaboration[a,*]

[a]*Univ. of Tsukuba,*
1-1-1 Tennoudai, Tsukuba, Japan

E-mail: sakai.shingo.gw@alumni.tsukuba.ac.jp

Electroweak bosons, $W^{\pm}$ and Z, are important observables in pp and heavy-ion collisions. In pp collisions, the measurements are useful for testing the perturbative QCD. In heavy-ion collisions, the measurements allow us to study the initial-stage effects, which are mainly due to modification of the parton distribution in the nucleus. In the ALICE experiment, the production of $W^{\pm}$ and Z is studied by exploiting their semileptonic decay channels in the wide rapidity region. In this contribution, the results in pp collisions at $\sqrt{s}$ = 13 TeV, p–Pb collisions at $\sqrt{s_{NN}}$ = 8.16 TeV and Pb–Pb collisions at $\sqrt{s_{NN}}$ = 5.02 TeV are reported.

---

[*]Speaker

1. Introduction

The $W^{\pm}$ and Z^0 bosons are powerful probes to study the quantum chromodynamics (QCD) in high-energy physics. They have large masses ($M_W = 80.379 \pm 0.012$ GeV/c^2 and $M_Z = 91.1876 \pm 0.0021$ GeV/c^2), and they are predominantly produced via quark-antiquark annihilation [1] [2] in early stage of pp and heavy-ion collisions. Therefore their production in pp collisions can be described by the perturbative QCD (pQCD). In addition, the production of W^+ and W^- is sensitive to the light quark parton distribution function and their asymmetry is reflected into the up-to-down ratio in the nucleon and nucleus [3]. In heavy-ion collisions, where the hot and dense QCD matter is created, $W^{\pm}$ and Z are unique probes because they do not interact with the medium constituents. Therefore they carry the information in the initial-state nuclear effects, such as the modification of the parton distribution functions (nPDFs) on nucleus, and provide new constrains to the nPDFs [3].

2. ALICE apparatus and W and Z bosons reconstruction

The analysis was performed using data recorded in pp collisions at $\sqrt{s} = 13$ TeV, p–Pb collisions at $\sqrt{s_{NN}} = 8.16$ TeV, and Pb–Pb collisions at $\sqrt{s_{NN}} = 5.02$ TeV with the ALICE detector. The details of the detectors and the performance are described in Ref [14]. The ALICE apparatus consists of central barrel detectors covering a range in pseudorapidity $|\eta| < 0.9$ and detectors at forward and backward rapidity. The central barrel detectors are placed in a uniform 0.5 T magnetic field along the beam axis supplied by the large solenoid magnet. In this analysis, the Inner Tracking System (ITS), the Time Projection Chamber (TPC) and the Electromagnetic Calorimeter (EMCal), located inside the central barrel are used for reconstructing and identifying electrons, while the muons are tracked and identified by the forward muon spectrometer, which covers the rapidity interval $2.5 < y < 4$. In p–Pb collisions, the center-of-mass system moves with $\Delta y = 0.465$ with respect to the laboratory frame in the proton-beam direction. The beam was switched during the p–Pb collisions, and the acceptance of the spectrometer is $2.03 < y_{cms} < 3.53$ (-4.46 < y_{cms} < -2.96) when the proton beam (the lead beam) moves towards the spectrometer.

At midrapidity, the $W^{\pm}$ boson candidates are reconstructed by measuring the electrons from their semileptonic decays. The electrons are selected based on their energy loss (dE/dx) in the TPC and the energy-to-momentum ratio ($E/p \sim 1$) where the energy was measured in the EMCal. Electrons with p_T larger than 40 GeV/c were used. In this p_T region, background is mainly composed by heavy-flavour hadrons and Z boson decays. The separation of W boson and heavy-flavour hadrons was performed by an isolation criterion that was tuned based on the energy information around the candidate electrons. The contribution of electrons from Z boson decays was estimated using the POWHEG simulation [4].

At forward rapidity, the $W^{\pm}$ boson candidates are reconstructed in the single-muon channels. The signal raw yield is extracted by fitting the measured single muon transverse momentum spectrum ($p_T^{\mu} > 10$ GeV/c) with the templates extracted using Monte Carlo simulations for the signal (muons from W boson decay) and background (muons from Z boson and heavy-flavour hadrons decays). The simulations for W and Z boson decays were performed with the event generator POWHEG [4], and for heavy-flavour hadrons were based on FONLL QCD calculation [11, 12]. In the POWHEG simulation for p–Pb and Pb–Pb collisions, the lead nucleus isospin was taken into account by

weighting the proton and neutron contributions. The Z bosons are reconstructed experimentally by the invariant mass in the dimuon decay channel $Z \rightarrow \mu^+ \mu^-$. The muon candidates are required to have $p_T > 20$ GeV/c in the rapidity range $-4 < \eta^\mu < -2.5$. Backgrounds from other semileptonic decays of $c\bar{c}$, $b\bar{b}$ and $t\bar{t}$ pairs and the muonic decay of τ pairs are estimated with MC simulations.

3. Results

3.1 W$^\pm$ production in pp collisions at $\sqrt{s}$ = 13 TeV

Figure 1 shows the p_T differential cross sections for electrons from W$^-$ (left) and positrons from W$^+$ (right) in $|y| < 0.6$ in pp collisions at $\sqrt{s}$ = 13 TeV. The measured cross sections are compared with POWHEG simulations [4] which are based on NLO pQCD. The CT10NLO PDFs [5] were used in these calculations, and the bands represent the theoretical uncertainty from the PDFs. The measured cross sections are consistent with the POWHEG calculations within experimental and theoretical uncertainties. The cross section ratio $\sigma(e^+ \leftarrow W^+)/\sigma(e^- \leftarrow W^-)$ was calculated and the result is shown in Fig. 2. There is a hint of a larger cross section for $e^+ \leftarrow W^+$ in data, which indicates the isospin effect on the W boson productions. However, the large uncertainties do not allow us to draw firm conclusions. The larger cross section for $e^+ \leftarrow W^+$ is also predicted by the POWHEG calculation, and the calculation is in good agreement with the measurement.
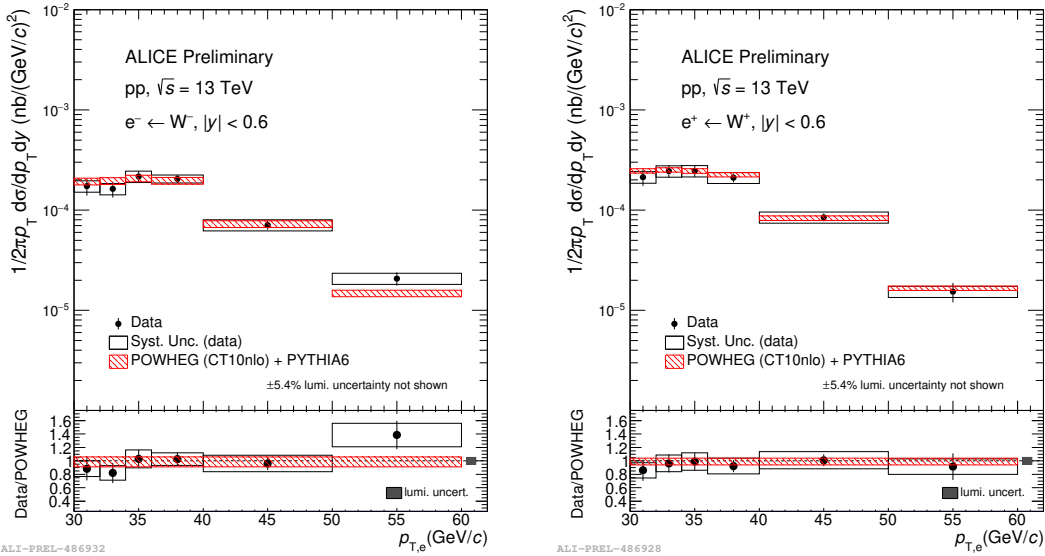

Figure 1: p_T-differential cross sections for electrons (positrons) from W$^-$ (W$^+$) at $\sqrt{s}$ =13 TeV. The red bands are POWHEG calculations with CT10NLO PDFs.

3.2 W$^\pm$ production in p–Pb collisions at $\sqrt{s}$ = 8.16 TeV and Pb–Pb collisions at $\sqrt{s_{NN}}$ = 5.02 TeV

Figure 3 (left) shows the lepton-charge asymmetry at forward and backward rapidity for muons from W boson decays. The result shows the clear asymmetry in forward and backward rapidity, and the result indicates that W$^+$ (u$\bar{d}$) (W$^-$ (d$\bar{u}$)) production is dominant in forward (backward) rapidity. The asymmetry is compared with model calculations based on pQCD (MCFM [6]) with and without
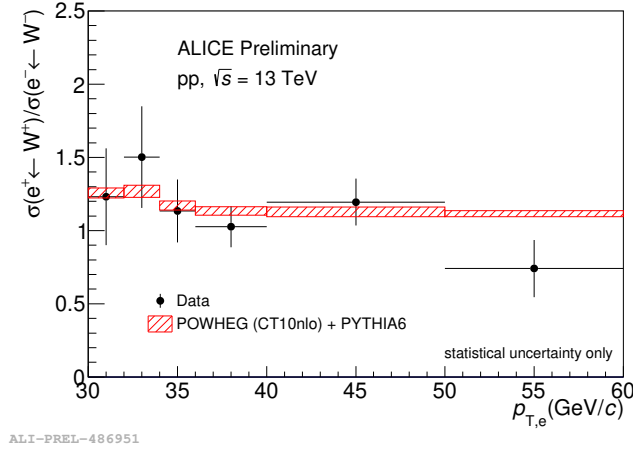
ALI-PREL-486951

Figure 2: Cross section ratio $\sigma(e^+ \leftarrow W^+)/\sigma(e^- \leftarrow W^-)$ as a function of p_T in pp collisions at $\sqrt{s} = 13$ TeV. The red bands are POWHEG calculations with CT10NLO PDFs.

the nuclear modification of the parton distribution functions (EPPS16 [8]). In the calculations, the proton and neutron contributions are weighted to reproduce the lead nucleus isospin. The models with and without nuclear modification reproduce the measured asymmetry at both forward and backward rapidity.

The $W^\pm$ boson production cross section in Pb–Pb collisions at $\sqrt{s_{NN}} = 5.02$ TeV normalized by the nuclear overlap function ($\langle T_{AA} \rangle$) as a function of the centrality is shown in Fig. 3 (right). The cross section for W^+ and W^- follows the $\langle T_{AA} \rangle$ scaling, which indicates that there are no final state effects, *i.e.*, energy loss, on the W productions. The difference between W^+ and W^- cross sections is caused by the isospin effect.

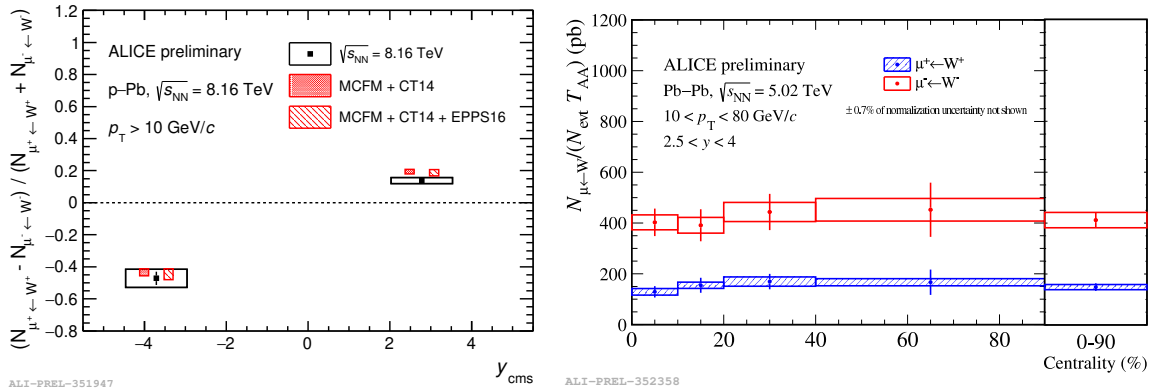ALI-PREL-351947   ALI-PREL-352358

Figure 3: (left) Lepton-charge asymmetry as a function of rapidity for muons from W boson decays in p–Pb collisions at $\sqrt{s_{NN}} = 8.16$ TeV. The result is compared with theoretical calculations with and without nuclear effects. (right) Normalized invariant yield of muons from W^+ and W^- as a function of the centrality in Pb–Pb collisions at $\sqrt{s_{NN}} = 5.02$ TeV.

3.3 *Z* production in p–Pb collision at $\sqrt{s}$ = 8.16 TeV and Pb–Pb collisions in $\sqrt{s_{NN}}$ = 5.02 TeV

Figure 4 (left) shows the production cross section of Z boson in p–Pb collisions at $\sqrt{s_{NN}}$ = 8.16 TeV [13]. The cross sections are measured at forward and at backward rapidity, and the results are compared with model calculations based on pQCD (MCFM [6] and FEWZ [7]) with and without the nuclear modification of the parton distribution functions (EPPS16 [8] and nCTEQ15 [9]). In the calculations, the proton and neutron contributions are weighted to reproduce the lead nucleus isospin. The cross sections measured at forward and backward rapidity are consistent with the pQCD calculations incorporating both free-nucleon and nuclear-modified PDFs.

The measurement in Pb–Pb collisions at $\sqrt{s_{NN}}$ = 5.02 TeV [13] is shown in Fig. 4 (right). The result is normalized by the nuclear overlap function. The result is also compared with the theoretical calculations based on MCFM and FEWZ with and without nuclear modifications (EPPS16, nCTEQ15 and EPS09s [10]). The calculations with nuclear modifications are in good agreement with data. On the other hand, the calculation without the modification (MCFM + CT14) is 3.4σ higher than the data.
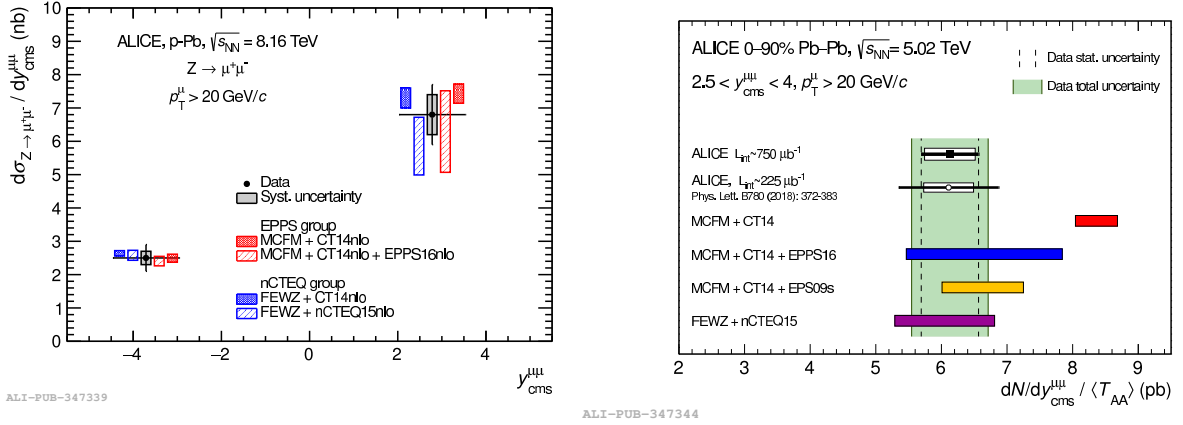

ALI-PUB-347339

ALI-PUB-347344

Figure 4: (left) Production cross section of $\mu^+\mu^-$ from Z boson decays in p–Pb collisions at $\sqrt{s_{NN}}$ = 8.16 TeV. The results are compared with theoretical calculations based on CT14 free-nucleon PDFs and on other PDF sets including the presence of a nuclear modification. (right) Production cross section of $\mu^+\mu^-$ from Z boson decays in Pb–Pb collisions at $\sqrt{s_{NN}}$ = 5.02 TeV. The cross section is normalized by the nuclear overlap function. The result is also compared to model calculations with and without nuclear modifications (EPPS16, nCTEQ15 and EPS09s).

4. Summary

The production of W and Z bosons was measured with the ALICE experiment in pp collisions at $\sqrt{s}$ = 13 TeV, p–Pb collisions at $\sqrt{s_{NN}}$ = 8.16 TeV and Pb–Pb collisions at $\sqrt{s_{NN}}$ = 5.02 TeV. In pp collisions, $W^{\pm}$ production was studied by measuring electrons from their decay at midrapidity ($|y|$ < 0.6). The measured cross sections for $e^{\pm} \leftarrow W^{\pm}$ and the cross section ratio are in good agreement with theoretical prediction based on pQCD. In p–Pb collisions, the cross sections for $\mu^{\pm} \leftarrow W^{\pm}$ and $Z \rightarrow \mu^+\mu^-$ were measured at forward and backward rapidity. The measurements were compared with the models with and without nuclear modification of the PDFs. In Pb–Pb

collisions, $\mu^{\pm} \leftarrow W^{\pm}$ and $Z \rightarrow \mu^+\mu^-$ were measured at forward rapidity. The Z production cross section is in good agreement with the model including the nuclear effects, whereas the model without these effect is 3.4σ higher than the data. The measured $\mu^{\pm} \leftarrow W^{\pm}$ cross sections scaled by the nuclear overlap functions indicate that the production of W is not affected by final state effects such as energy loss in the quark-gluon plasma. The sizeable amount of new measurements at large rapidities provide extra inputs for nPDSs global fits [3].

References

[1] S. D. Drell and T. M. Yan, Phys. Rev. Lett. **25** (1970), 316-320 [erratum: Phys. Rev. Lett. **25** (1970), 902]

[2] A. H. Ajjath, G. Das, M. C. Kumar, P. Mukherjee, V. Ravindran and K. Samanta, JHEP **10** (2020), 153

[3] H. Paukkunen and C. A. Salgado, JHEP **03** (2011), 071

[4] S. Alioli, P. Nason, C. Oleari and E. Re, JHEP **07** (2008), 060

[5] H. L. Lai, M. Guzzi, J. Huston, Z. Li, P. M. Nadolsky, J. Pumplin and C. P. Yuan, Phys. Rev. D **82** (2010), 074024

[6] R. Boughezal, J. M. Campbell, R. K. Ellis, C. Focke, W. Giele, X. Liu, F. Petriello and C. Williams, Eur. Phys. J. C **77** (2017) no.1, 7

[7] R. Gavin, Y. Li, F. Petriello and S. Quackenbush, Comput. Phys. Commun. **182** (2011), 2388-2403

[8] K. J. Eskola, P. Paakkinen, H. Paukkunen and C. A. Salgado, Eur. Phys. J. C **77** (2017) no.3, 163

[9] K. Kovarik, A. Kusina, T. Jezo, D. B. Clark, C. Keppel, F. Lyonnet, J. G. Morfin, F. I. Olness, J. F. Owens and I. Schienbein, *et al.* Phys. Rev. D **93** (2016) no.8, 085037

[10] I. Helenius, K. J. Eskola, H. Honkanen and C. A. Salgado, JHEP **07** (2012), 073

[11] M. Cacciari, M. Greco and P. Nason, JHEP **9805** (1998) 007 [arXiv:hep-ph/9803400].

[12] M. Cacciari, S. Frixione and P. Nason, JHEP **0103** (2001) 006 [arXiv:hep-ph/0102134].

[13] S. Acharya *et al.* [ALICE], JHEP **09** (2020), 076

[14] K. Aamodt *et al.* [ALICE], JINST **3** (2008), S08002